

Transient-liquid-phase and liquid-film-assisted joining of ceramics

Joshua D. Sugar^{a,b}, Joseph T. McKeown^{a,b}, Takaya Akashi^{a,b}, Sung M. Hong^{a,b},
Kunihiko Nakashima^c, Andreas M. Glaeser^{a,b,*}

^a Department of Materials Science and Engineering, 319 Hearst Mining Building, MC1760 University of California, Berkeley, CA 94720-1760, USA

^b Ceramic Science Program, Materials Sciences Division, Lawrence Berkeley National Laboratory, Berkeley, CA 94720-1760, USA

^c Department of Materials Science and Engineering, Faculty of Engineering, Kyushu University 36,
Hakozaki 6-10-1, Higashi-ku, Fukuoka 812-81, Japan

Available online 15 August 2005

Abstract

Two joining methods, transient-liquid-phase (TLP) joining and liquid-film-assisted joining (LFAJ), have been used to bond alumina ceramics. Both methods rely on multilayer metallic interlayers designed to form thin liquid films at reduced temperatures. The liquid films either disappear by interdiffusion (TLP) or promote ceramic/metal interface formation and concurrent dewetting of the liquid film (LFAJ). Progress on extending the TLP method to lower temperatures by combining low-melting-point (<450 °C) liquids and commercial reactive-metal brazes is described. Recent LFAJ work on joining alumina to niobium using copper films is presented.

Published by Elsevier Ltd.

Keywords: Joining; Interfaces; Fracture; Strength; Al₂O₃

1. Introduction

Joining is a critical enabling technology, essential to widespread use of ceramics in many applications. Specifically, it allows the fabrication of large, complex, multi-material, multifunctional assemblies through the controlled integration of smaller, less complex, more easily manufactured parts. Additionally, it can provide an avenue for repair of damaged structures through the replacement of defective components. This can extend the lifetimes of assemblies, and permit the reuse of components that are not readily recycled, e.g., fiber-reinforced materials.

Material degradation during joining and interfacial reactions that produce undesirable and structurally defective reaction layers can limit the properties and reliability of joined assemblies. The extent of degradation or reaction often increases with increasing joining temperature. Thus, when materials that are nanostructured and prone to coarsening, are amorphous and may crystallize, or otherwise have temperature-sensitive properties are part of a joined assembly,

it becomes increasingly important to reduce the joining temperature below some critical threshold temperature to mitigate such problems. Concurrently, it may be necessary to maintain the potential for service at temperatures that approach this critical threshold temperature.

Our research focuses on developing joining methods that yield reliably strong interfaces at “low” joining temperatures, but exploit multilayer interlayer designs that preserve the potential for use at temperatures that equal or exceed the joining temperature. An illustrative example of an assembly is shown in Fig. 1. The cladding layers are designed to form thin liquid layers at “low” temperatures. The core layer remains solid during joining. In transient-liquid-phase (TLP) joining, the overall composition of the interlayer lies in a solid solution phase field. Thus, the liquid is not stable and disappears due to interdiffusion. While the (transient) liquid is present, it fills interfacial gaps and facilitates joint formation. The remelt temperature of the homogenized interlayer exceeds the original joining temperature. Alternatively, the liquid film can be chemically stable but morphologically unstable. In this case, a thin liquid film interspersed between a ceramic and a solid core layer can promote rapid diffusion and the development of intimate contact between the ceramic

* Corresponding author. Tel.: +1 510 486 7262; fax: +1 510 643 5792.
E-mail address: aglaeser@sapphire.berkeley.edu (A.M. Glaeser).

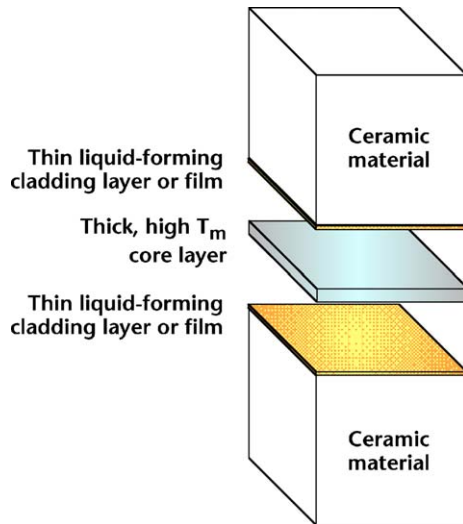


Fig. 1. Schematic illustration of an assembly with a multilayer interlayer. Two relatively thin cladding layers that form a liquid at low temperature flank a thicker and higher melting point core layer that dominates the composition and ultimate physical properties of the interlayer.

and core layer metal. Growth of ceramic–core layer contact progressively decreases the area fraction of liquid along the interface. This approach is referred to as liquid-film-assisted joining (LFAJ).

In this paper, we summarize prior research using TLP joining and describe ongoing efforts to extend the TLP method to lower temperatures by combining low-melting-point (<450 °C) cladding materials and commercial reactive-metal brazes. We also describe recent LFAJ work on joining alumina to niobium core layers using copper films. Effects of joining temperature, time, film thickness, and surface roughness on joint properties and interfacial microstructure evolution are presented.

2. Background

Several methods for ceramic-to-ceramic, metal-to-metal and ceramic-to-metal joining are available, and have been reviewed in the literature.^{1–5} A brief overview follows.

2.1. Conventional joining approaches

One class of joining processes, exemplified by diffusion bonding, involves purely solid-state processing.^{1,3–12} The components to be joined can be brought into direct contact or, as is often the case for ceramic–ceramic joining, a metallic foil can be inserted between the ceramic components. Application of a pressure at elevated temperature promotes the formation of a bonded interface between the materials to be joined. The temperatures required for joining are often a high fraction of the melting temperature of the least refractory component due to the need to activate

solid-state diffusion.^{1–9,11,13–15} Component deformation and microstructural changes such as grain growth or precipitate coarsening within the components can degrade properties.

A broader range of processes involves melting either the material(s) to be joined, or some other material introduced into the joint region.^{1,2,4,5,16} Examples include soldering, brazing, and welding. Solders, by definition, melt at <840 °F (<450 °C). As a result, the joints have limited temperature capability, and can be mechanically inferior to the bulk materials that have been joined. Brazes require higher processing temperatures (>840 °F). The higher melting temperatures of brazes can lead to higher service temperatures; however, the higher processing temperatures can overlap with the aging temperatures of some metallic alloys, resulting in a loss of peak hardness. Other forms of microstructural degradation are also possible. Welding involves localized heating, melting, and subsequent solidification. A major concern in welding of metals is the development of a heat-affected zone. Although metal–metal welding is common, and ceramic–ceramic welding has been explored, examples of ceramic–metal bonding via welding are sparse.

2.2. Nonconventional joining approaches

2.2.1. Transient-liquid-phase joining

TLP joining has been applied to a range of structural metals,^{17–22} notably nickel-base superalloys, and more recently the method has been extended to intermetallics.^{23–25} Reviews of this process are available in the literature.^{21,22} When applied to metal–metal joining, an interlayer containing a melting point depressant (MPD) is placed between the two objects to be joined. Boron serves as an effective MPD for nickel, and is thus a common interlayer component when nickel-base superalloys are joined.^{17–20} At the joining temperature, rapid (interstitial) diffusion of boron into the adjoining (boron-free) nickel-base superalloys leads to a progressive decrease in the amount of liquid. Ultimately, the liquid disappears. Counter-diffusion of alloying elements in the nickel-base superalloys into the interlayer region leads to joint chemistries and properties that approach those of the base material, and such joints are compatible with use in structural applications at elevated temperature.

When the method is extended to facilitate ceramic joining by metallic interlayers, the disappearance of the liquid generally requires diffusion of a low-melting-point metal that acts as an MPD into an adjoining solid phase. For the systems explored in our work, incorporation of the MPD into the ceramic is slow in comparison to diffusion into the solid core layer of the multilayer interlayer, and hence this latter diffusion path controls the rate of liquid disappearance.

Formation of successful joints by this approach requires that the liquid can flow along the interface to fill gaps, and that sufficient liquid is available for complete gap filling. Gaps along the interface are likely to arise due to roughness and waviness of the substrate surfaces, local depressions or asperities on the surfaces, and incomplete coating of the substrate

(or core layer) with the MPD-containing layer. In conventional brazing and soldering, if two ceramic components are to be joined, then it is the contact angle of the liquid braze or solder on the ceramic that will determine whether the liquid will recede from (enlarge) or advance into (fill) an interfacial gap. In the case of multilayer metallic interlayers, the liquid film is sandwiched between two dissimilar materials, the metal core and the ceramic. Thus, two contact angles, and more specifically their sum,²⁶ will dictate the (short-time) response of the liquid. The surface topography will modify the energetic considerations, and also impact the liquid film thickness required to fill interfacial voids.

In Fig. 2a, a film is shown between two dissimilar but parallel substrates. The contact angle on the core layer, θ_1 , is shown to be acute, as would normally be the case for a metal on a metal, while the contact angle on the ceramic, θ_2 , is shown as obtuse, as would normally be the case for nonreactive metals on ceramics. The liquid film will fill voids if $\theta_1 + \theta_2 < 180^\circ$. If a typical liquid metal (with $\theta > 90^\circ$) were sandwiched between two ceramic substrates, the liquid would “dewet” the interface, introduce significant porosity, and lead to nonhermetic low-strength joints. Thus, one of the advantages of a multilayer interlayer approach is that a high θ_2 is permissible, if θ_1 is sufficiently low. When $\theta_1 + \theta_2 < 180^\circ$, it implies that, $\gamma_{\text{Core/Liq}} + \gamma_{\text{Liq/Ceramic}} < \gamma_{\text{Core/Vapor}} + \gamma_{\text{Ceramic/Vapor}}$ where $\gamma_{i/j}$ is the specific surface or interfacial energy of the i/j interface.

When the bonding surfaces are rough, a more stringent condition emerges. If the contact angles of liquid on the core layer and the ceramic are again denoted θ_1 and θ_2 , respectively, but local depressions on the opposing core layer and ceramic surfaces cause angular deviations of α_1 and α_2 , respectively, from a parallel surface geometry, then flow of liquid into voids will only occur if the condition $(\theta_1 + \alpha_1) + (\theta_2 + \alpha_2) < 180^\circ$ is met. Since θ_1 and θ_2 can vary as the surface orientations and surface energies of the metal and ceramic grains vary, and α_1 and α_2 will vary with location along the interface, the potential exists for regions of the interface with diverging surfaces ($\alpha_1 + \alpha_2 > 0$) to have unfavorable wetting conditions. A rougher surface with locally larger values of α_1 and α_2 would be more likely to contain

voids that persist or develop due to liquid film redistribution. In addition, spatial variations in $(\theta_1 + \alpha_1) + (\theta_2 + \alpha_2)$ could establish conditions that redistribute the liquid from filled regions where the sum is higher into unfilled regions where the sum is lower, thereby generating interfacial flaws.

When properly implemented, TLP joining methods are capable of producing joined assemblies with reproducible and robust joint properties. When incomplete wetting occurs, regions of the interface remain or become liquid-free, and a triple-junction ridge develops where the liquid metal, ceramic, and vapor phases form mutual contact. Fractography indicates that these regions are more prevalent in samples with lower fracture strength.^{26–29} The wetting characteristics of the liquid film can be improved by precoating the ceramic surface with a metal, or by altering the liquid film chemistry.^{30–34} The liquid film chemistry can be adjusted by adding directly to the cladding layer a second component that improves wetting. Alternatively, since some dissolution of the core layer is inevitable, the addition of elements that enhance the wetting can be achieved by their incorporation in the core layer. In some of the systems examined, the implementation of such approaches has yielded assemblies in which fracture occurs primarily within the ceramic, indicating that the ceramic–metal interface has higher strength than the ceramic.³⁴

2.2.2. Liquid-film-assisted joining

In LFAJ, as in TLP bonding, a thin liquid film is sandwiched between a solid metal core layer and the ceramic to be joined. Gap filling is again an issue. Thus, the same energetic issues that apply in TLP bonding, illustrated in Fig. 2a, are relevant. When, $(\theta_1 + \alpha_1) + (\theta_2 + \alpha_2) < 180^\circ$ the liquid will fill gaps. However, in contrast to TLP joining, in LFAJ the liquid former does not have significant solubility in the core layer, and thus, the liquid phase does not disappear with time. However, at longer times, other microstructural changes (that may require more sluggish solid-state diffusion) can occur. The continuous liquid metal film is initially bounded by two interfaces, one with the core layer and the other with the ceramic. It follows that if $\gamma_{\text{Core/Ceramic}} < \gamma_{\text{Core/Liq}} + \gamma_{\text{Liq/Ceramic}}$, it would be energetically favorable to break up the liquid film and form

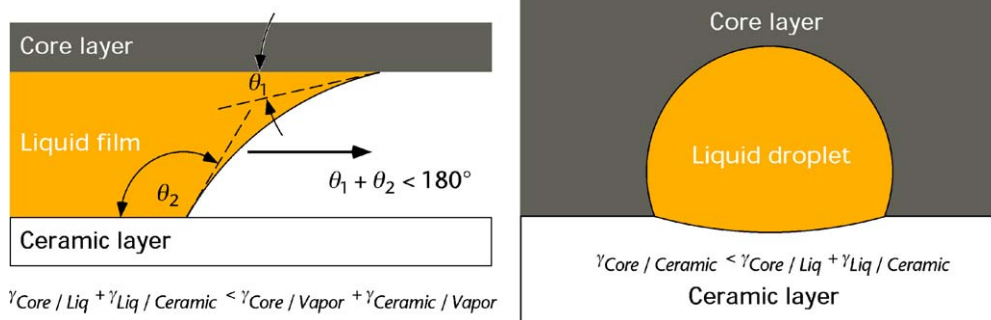


Fig. 2. (a) Schematic illustration of a thin liquid film sandwiched between a solid metallic core layer and a ceramic on which the liquid has contact angles θ_1 and θ_2 , respectively. For parallel core layer and ceramic surfaces, void filling requires that $\theta_1 + \theta_2 < 180^\circ$. (b) In LFAJ, at later stages, liquid-film-assisted growth of ceramic–core contact produces a “dewetting” of the ceramic–core layer interface and results in isolated droplets of liquid.

discrete particles. “Dewetting” of the film does not involve the generation of interfacial voids. Instead, in LFAJ the retraction and instability of the liquid film is accompanied by the growth of ceramic–core layer interface. In the presence of the liquid film, grain boundaries in both the core layer and the ceramic are etched, and for diffusional growth of the grain boundary grooves, ridges can form that extend above the original surface. When the ridge heights become sufficiently large, the ridge crests contact the adjoining phase. Grain boundary grooving can initiate ceramic–core layer contact, producing microstructures like those shown in Fig. 3a. With increasing anneal time, the area fraction of ceramic–core layer contact increases and can ultimately exceed 90%, as illustrated in Fig. 3b and c, respectively.

2.2.3. Results of TLP and LFAJ approaches

A large number of multilayer interlayer systems have been developed and used to join alumina and silicon-based ceramics. In general, the low-melting-point component of the interlayer has been copper and core layers with melting points several hundred degrees higher have been used. Examples of multilayer interlayers used to join alumina include: Cu/Pt/Cu,²⁷ Cu/Ni/Cu,²⁸ Cr/Cu/Ni/Cu/Cr, and Cu/80Ni20Cr/Cu.^{32,35} Similar strategies have been employed in bonding silicon-based ceramics.^{30,31,33,36} Ceccone et al.³³ have explored the use of Au/80Ni20Cr/Au interlayers for TLP bonding of silicon nitride. Silicon nitride^{30,31} and silicon carbide³⁰ were also joined using a Cu–Au/Ni/Cu–Au-based interlayer designed to form a liquid phase at <950 °C. Changes in processing conditions, specifically the processing temperature, were found to have a strong effect on silicon nitride joint properties.³¹ A plot summarizing strength distributions for various interlayer and ceramic combinations is provided in Fig. 4. Data for silicon carbide is omitted for clarity, but can be found in reference.³⁰ A key point is that reliably strong joints can be produced with interlayer chemistries compatible with higher service temperatures than those typical of many commercial reactive-metal brazes.

3. Experimental procedures

The sample preparation procedures in our current work are generally similar to those in our prior work, and detailed descriptions are available in the literature.^{26–32,34–39} The summary provided here emphasizes those procedures or materials that differ from those used previously.

3.1. Materials and sample preparation

Commercially available 99.5% pure (AD995, Coors Technical Ceramic Co., Oak Ridge, TN) or 99.9% pure (SSA-999W, Nikkato Corp., Osaka, Japan) aluminum oxide in the form of 19.5 mm × 19.5 mm × 22.5 mm blocks was used for assemblies intended for mechanical testing. The finer grain size 99.9% alumina has a higher fracture strength, but

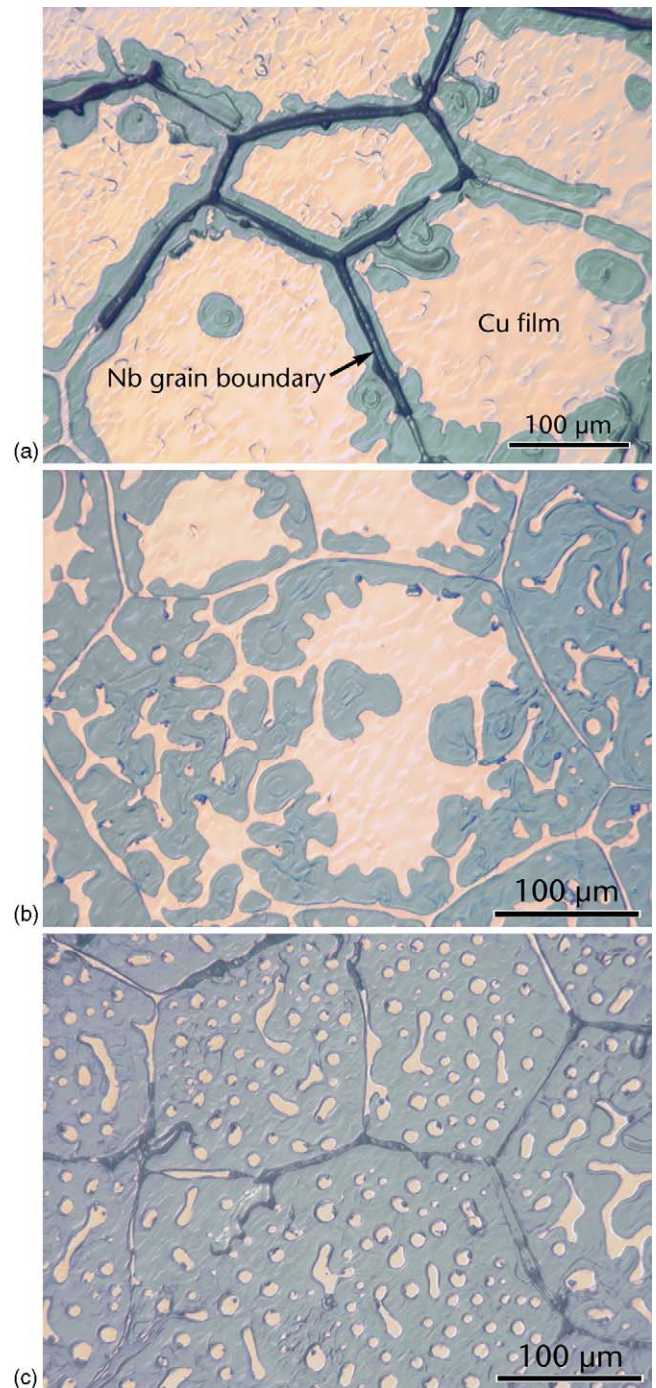


Fig. 3. Optical micrographs taken of a sapphire/copper/niobium interface showing (a) initial, (b) intermediate, and (c) final stages of sapphire–niobium contact growth. Note that in the final stage, sapphire–niobium contact dominates the interface microstructure ($\approx 90\%$ area fraction), and therefore the thermomechanical characteristics of the interface.

its properties can be affected by the thermal cycle during joining.²⁹ The joining surfaces of the blocks were ground flat on a surface grinder using a 400-grit diamond wheel. Joints processed with unpolished alumina substrates were then cleaned while those processed with polished alumina

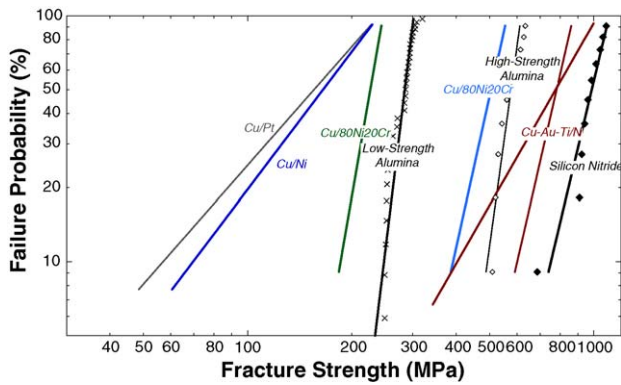


Fig. 4. Room-temperature strength distributions for different interlayer designs used to join alumina and silicon nitride. Cu/Pt, Cu/Ni, and Cu/80Ni20Cr interlayers were used to bond alumina. Note the beneficial effect of Cr additions. The Cu–Au–Ti/Ni interlayer was used to bond silicon nitride; the two lines correspond to different joining temperatures.

substrates were polished with progressively finer grit size diamond suspensions (South Bay Technologies, San Clemente, CA) before cleaning. After polishing with a 1- μm diamond suspension, either a final chemical–mechanical polish was performed using colloidal silica (Struers, Westlake, OH), or a final mechanical polish using 0.25- μm grit diamond paste was performed. Samples to investigate interfacial microstructure evolution were fabricated using ≈ 0.5 -mm-thick, high-purity, optical finish, *c*-axis or *m*-axis sapphire substrates (Crystal Systems Inc., Salem, MA) that required no additional polishing.

For brazing and TLP joining, 75- μm -thick, 99.95% pure silver foils (Alfa Aesar, Ward Hill, MA) and silver-based reactive-metal braze foils, Silver ABA (Morgan Advanced Ceramics, Belmont, CA), were used. In the TLP bonding experiments, a $>99.998\%$ pure indium source (Alfa Aesar, Ward Hill, MA) was used to develop cladding layers. For the LFAJ experiments, a flattened and cleaned, 99.99% pure, 127- μm thick niobium foil (Goodfellow Corp., Malvern, PA) provided the core layer and a commercial grade copper (Consolidated Companies Wire and Associated, Chicago, IL) served as the basis for the cladding film. Both the indium and the copper were deposited directly onto the alumina surfaces by melting the source material and allowing it to evaporate in a high-vacuum chamber containing the ceramic blocks. Film thicknesses were measured using profilometry (Tencor Instruments Inc., San Jose, CA) and weight-gain measurements.²⁷ The combined thickness of the indium film and a very thin capping layer of 99.9% pure silver (designed to prevent indium oxidation) was ≈ 2.2 μm . The multilayer interlayer has an overall composition (in wt%) of 89.1% Ag, 4.8% Cu, 3.9% In, 1.2% Ti, and 1.0% Al. For bonds prepared with niobium core layers, samples with 1.4-, 3.0-, and 5.5- μm thick copper films were prepared.

All bonding was performed in a vacuum hot press. Brazing with pure silver and with Silver ABA was performed at 1000 and 960 °C for 10 min, respectively; silver melts at 960 °C, while the liquidus temperature of Silver ABA is 912 °C. TLP

bonding with an indium cladding was performed at 700 and 800 °C, below the Silver ABA solidus temperature of 860 °C with holding times varying from as little as 20 min up to 24 h. Typical heating rates and cooling rates were 10 °C/min and 8 °C/min, respectively, with a typical vacuum of $<10^{-7}$ atm and an applied load of ≈ 4.6 MPa.

For polycrystalline alumina joined with Cu/Nb/Cu interlayers, assemblies were processed with a vacuum pressure below 10^{-7} atm, an applied load of ≈ 2.2 MPa, a heating rate of 4 °C/min, a 6 h soak at 1400 °C, and cooling at 2 °C/min. To study microstructural evolution at the interface, sapphire was used as an optically transparent surrogate for polycrystalline alumina, and bonds were made at 1150 °C using the same heating and cooling rates, dwell time, and load. Most sapphire samples were annealed at 1150 °C rather than 1400 °C to decrease the rate of interface evolution and permit a more detailed study of the kinetics.

4. Characterization

To allow a comparison between the surface roughness of the ceramic substrates and the cladding film thickness the surface roughness of the as-ground and polished alumina blocks was determined by atomic force microscopy (AFM).^a The AFM scans typically covered a 50 $\mu\text{m} \times 50$ μm area, and provided accurate measurements of the local fine-scale roughness. To assess longer wavelength (and larger amplitude) variations in the surface topography, profilometer scans spanning ≈ 1 cm lengths were also conducted on polished and as-ground alumina. For the ground alumina, scans were taken both parallel and perpendicular to the grinding direction.

After bonding, the assemblies were machined into beams ≈ 3 mm \times ≈ 3 mm in cross section and ≈ 4 cm in length, with the metal interlayer at the center of the beam. The tensile surfaces of the beams were polished to a 1- μm finish and the beam edges were beveled to remove machining flaws that could initiate failure. This allowed for a more meaningful measurement of the fracture strength of the joined assembly, and the observed fracture path provided insight on the relative strengths of the ceramic–metal interface and the bulk ceramic. Beams were tested at room temperature using four-point bending.

The interlayer region of intact beams and the fracture surfaces of failed beams were examined using optical microscopy to assess the interlayer microstructure and the area fraction of ceramic–interlayer contact. Studies of interfacial microstructure evolution during LFAJ also utilized optical microscopy. Fiducial marks produced on the outer surfaces provided reference points allowing the same interfacial region to be identified after varying periods of annealing,

^a Measurements were also performed on the niobium foil, but the surface finish of the niobium was constant in the experiments, and since some dissolution of niobium occurs, the niobium surface roughness will change during bonding.

thereby providing a time sequence. Image analysis of the digital images allowed a determination of the area fraction of copper at the interface for given annealing conditions. Numerous samples and regions were analyzed.

5. Results and discussion

5.1. Transient-liquid-phase joining

Silver dissolves a significant amount of indium over a wide range of temperature.⁴⁰ It was thus of interest to assess whether silver-rich interlayers could be produced in situ and used to bond alumina when indium serves as the low-melting-point cladding layer. Brazing experiments using pure silver foils, and TLP experiments with pure silver core layers and indium cladding layers were performed. Neither interlayer produced useful joints. Silver forms an obtuse contact angle on alumina⁴¹ and was therefore expected to dewet the interface. Indium reportedly forms a high contact angle on alumina,⁴² and thus, it was expected that the silver–indium combination would also be problematic. In practice, assemblies were not sufficiently robust to survive machining into plates and beams.

It had been anticipated that the wetting of the liquid film on alumina would need improvement. In prior work by Nakashima and co-workers^{32,34} alumina joints prepared with Cu/Ni/Cu interlayers failed exclusively along the alumina–interlayer interface, and the joint strengths varied considerably. Examination of fracture surfaces indicated that large unbonded regions persisted along the alumina–interlayer interface. The results suggested that these flaws were involved in failure initiation, and that the statistical variations in these flaw sizes contributed to the wide strength distribution. Chromium additions were shown to reduce the contact angle of molten copper on alumina. By replacing a pure nickel core layer with an 80Ni20Cr core layer, dissolution of the core layer during joining added chromium to the liquid film. The significant improvement in joint characteristics achieved with a 80Ni20Cr core layer encouraged a parallel approach for silver–indium interlayers.

Numerous researchers have used copper–silver eutectic brazes with reactive-metal additions (i.e., Cusil ABA) to successfully join alumina (see for example reference²). Key to the success of these brazes is the addition of titanium, which promotes wetting of an otherwise nonwetting eutectic liquid. The copper–silver eutectic temperature is 780 °C. Incusil ABA is an interesting derivative of these brazes. Incusil ABA contains 12.5% indium, which lowers the liquidus temperature (715 °C), and 1.25% titanium, which promotes wetting. Incusil ABA has also been used to successfully join alumina. This suggests that the copper-rich and silver-rich phases in this alloy, which contain indium and titanium, form strong interfaces with alumina.

Joining experiments using thin indium cladding layers with Silver ABA have produced successful joints, and results

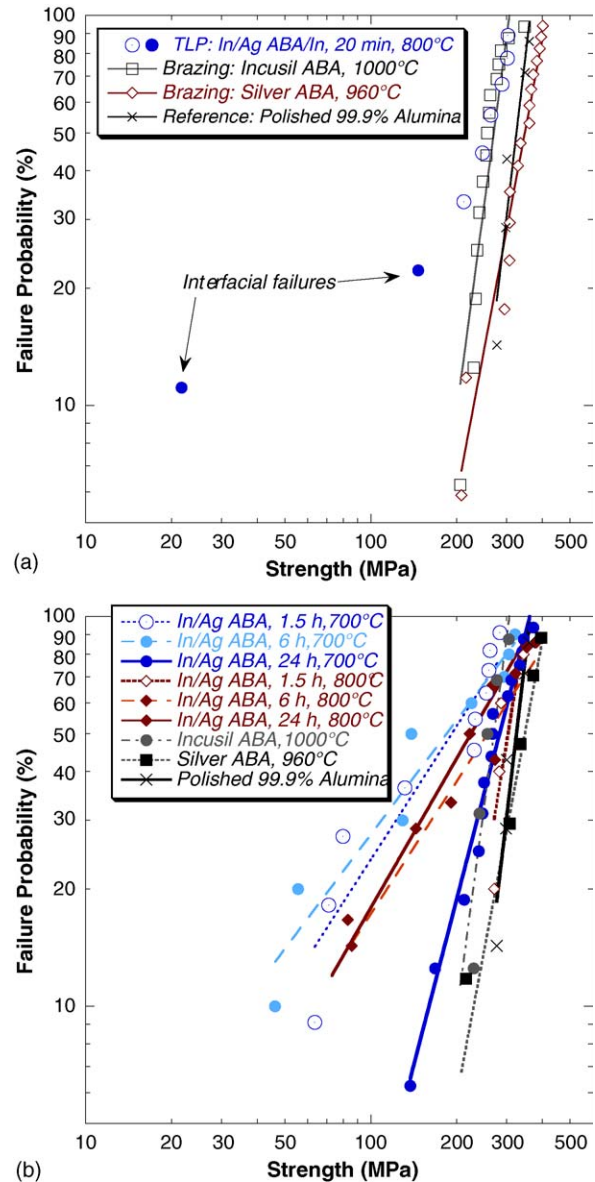


Fig. 5. Plots of fracture probability vs. fracture strength for alumina joined using In/Silver ABA/In interlayers. (a) 20 min bonding cycle at 800 °C, and comparison to conventional reactive-metal brazing. (b) Effect of bonding time and temperature on strength and failure characteristics of TLP bonds.

are summarized in Fig. 5. To provide a basis for comparison, samples were brazed using Silver ABA and Incusil ABA. For Silver ABA, the average four-point bend strength was 330 MPa, with a standard deviation of 60 MPa; for Incusil ABA, the corresponding values were 260 and 35 MPa. The as-received alumina had an average fracture strength of 320 MPa with a standard deviation of 30 MPa. Although most brazed samples failed in the ceramic, some samples failed along the alumina–interlayer interface, while others showed mixed ceramic and interfacial fracture paths. In samples brazed using In/Silver ABA/In interlayers, at elevated bonding temperatures, indium will melt and incorporate both silver and titanium from the Silver ABA core layer. Since the liquid film

is silver-rich, it will be substantially thicker than the original indium cladding layer. For bonds formed at 800 °C, with hold times of 20 min, the average fracture strength for samples that failed in the ceramic (270 ± 35 MPa) was comparable to those of samples brazed with Incusil ABA. However, low-stress interfacial failures were also observed. An examination of fracture surfaces of the weak beams suggested incomplete contact between the interlayer and the ceramic.

Varying the bonding time (1.5, 6, and 24 h) and temperature influenced the strength distributions. For samples bonded at 700 °C, maximum average strength and minimum standard deviation was attained after a 24-h hold. For samples bonded at 800 °C, the best results were obtained after a 1.5-h hold. In contrast to brazing, where all the titanium in the interlayer is available to form reaction layers, in TLP bonding, the total amount of titanium in each liquid film is smaller. It is possible that solid-state diffusion of titanium to the interface plays a role in the variations in strength. Further study will be required to assess this possibility. However, considering that the core layer compositions are optimized for brazing rather than TLP bonding, the results are very encouraging, and studies involving Copper ABA and Cusil ABA core layers are in progress. Results of these studies and a more complete account of work involving Silver ABA interlayers will be published elsewhere.

5.2. Liquid-film-assisted joining

Multilayer interlayers based on the copper-niobium system have been used to implement LFAJ, and the use of Cu/Nb/Cu interlayers for joining alumina has been studied extensively.^{26,29,39,43,44} A thin copper-rich film has a desirably low melting temperature (relative to niobium). The phase diagram of the copper-niobium binary system has only one reaction isotherm, a shallow eutectic near the copper-rich side of the diagram.⁴⁰ The solubility of copper in solid niobium is low. In view of the high melting temperature of niobium, and the fact that copper is a substitutional impurity, the rate of copper diffusion into niobium is also expected to be low at modest temperatures. Thus, the copper-rich liquid that will coexist with niobium at temperatures above the eutectic temperature will be a “permanent” feature of the interlayer microstructure. At 1150 °C, the niobium-saturated liquid contains ≈ 0.9 at% niobium while at 1400 °C it contains ≈ 1.7 at% niobium. The liquid film provides a high diffusivity pathway for niobium that allows the formation of extensive alumina-niobium contact (an area fraction $\geq 90\%$) along the alumina-interlayer interface,^{26,29,39,43} as illustrated in Fig. 3.

The energetics of the process lead to a breakup of the continuous film (described as dewetting) and the formation of discrete copper-rich droplets along the alumina-interlayer interface^{26,29,39,43} that enhance interfacial toughness by undergoing ductile tearing when the failure propagates along the interface.⁴⁴ When properly implemented the average fracture strength of the bonded assemblies is $\approx 90\%$ of the average fracture strength of the alumina that

was bonded, and the standard deviations in strength for the joined and reference assemblies are comparable.^{29,39,43} It is important to note that even at elevated temperatures, above the melting point of the dispersed phase (≈ 1080 °C), the joints retain a significant fraction of their room temperature strength; loss of strength reflects in large part the strength loss of the alumina due to softening of an intergranular glassy film,²⁹ and partly the drop in the yield strength of the copper particles.

Experimental studies of film breakup at polycrystalline alumina-interlayer interfaces are difficult because the interface cannot be examined nondestructively. Copper distributions in samples that undergo alumina-interlayer interfacial failure are not necessarily representative. Using sapphire allows the interfacial microstructure to be observed and recorded, and by examining the same region of the interface after varying anneal times, a time sequence can be constructed. Optical micrographs were taken at various regions of sapphire-interlayer interfaces, and image analysis was used to assess the area fraction of copper at the interface as a function of anneal time at 1150 °C. A limited number of samples were (bonded and) annealed at 1400 °C. Multiple contact initiation sites and multiple mechanisms (asperity contact and growth, grain boundary grooving, surface instability) can contribute to contact formation and liquid redistribution. The scaling behavior of competing mechanisms can differ, and thus variations in the dominant mechanism will manifest themselves by different scaling law exponents.

Efforts were made to fit the evolution behavior to a Johnson–Mehl–Avrami equation of the form:

$$f = 1 - \exp(-kt^n)$$

where f is the volume fraction of transformed material, k a kinetic parameter, t time, and n an exponent typically between 1 and 4. In this case, sapphire-copper contact transforming into sapphire–niobium contact is interpreted as the phase transformation and f is the area fraction of sapphire–niobium contact. The curves generated from fitting the data to this model are shown in Fig. 6a and b for samples with ≈ 3 - μm thick films annealed at 1150 and 1400 °C, respectively. The effect of temperature on the kinetics is evident. Samples bonded and then annealed at 1150 °C had values of k and n ranging from 0.045254 to 1.0102 and 0.253385 to 0.78828, respectively. The data was divided into three subsets representing rapid, “average”, and slow transformation. For the “average” interface, values of k and n were 0.4062 and 0.417399, respectively, which yields the middle curve in Fig. 6a, and represents the majority of the overall data. At 1400 °C values of k and n ranged from 1.3645 to 2.3082 and 0.47525 to 0.71082, respectively. The variable n in the Johnson–Mehl–Avrami equation is sensitive to the dimensionality of the transformation being modeled, and it largely affects the shape of the model curve. The large variation in n for data at one temperature is consistent with the interpretation that the mechanism dominating film breakup can vary with position at the interface.

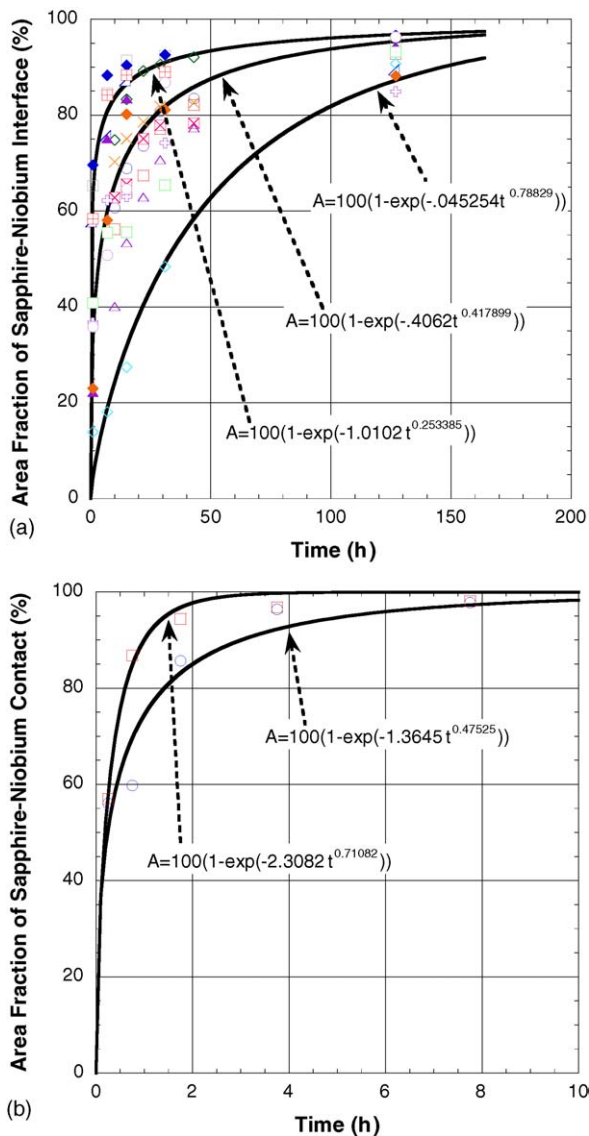


Fig. 6. Assessment of the “dewetting” kinetics for the copper film in LFAJ. At 1150 °C, the area fraction of sapphire–niobium contact increases rapidly and typically exceeds 80% after 10–20 h. At 1400 °C, the area fraction of sapphire–niobium contact exceeds 90% after just a few hours.

The roughness of the bonding surfaces is another factor that plays an important role in liquid redistribution, film breakup, and ultimate joint properties. One measure of roughness is the average roughness, R_a , defined as:

$$R_a = \left(\frac{1}{L} \right) \int_0^L f(x) dx$$

where L is the length of the measured distance and $f(x)$ the distance to the surface measured from the centerline. When surfaces are highly polished and R_a is small, thinner films with more rapid breakup kinetics may be adequate to fill interfacial gaps, but toughening contributions may be decreased. When R_a is large, a thicker film may be required for gap filling. Thick films may leave larger patches of relatively weaker alumina–copper contact along the interface.

Prior work, conducted using highly polished sapphire wafers or highly polished polycrystalline alumina substrates, showed that the introduction of a thin copper film improved the strength characteristics relative those obtained using solid-state diffusion bonding with the same time–temperature–load cycle. Results of these studies are summarized in Fig. 7a for samples bonded at 1400 °C (6 h, 2.2 MPa). Experiments were repeated using as-ground alu-

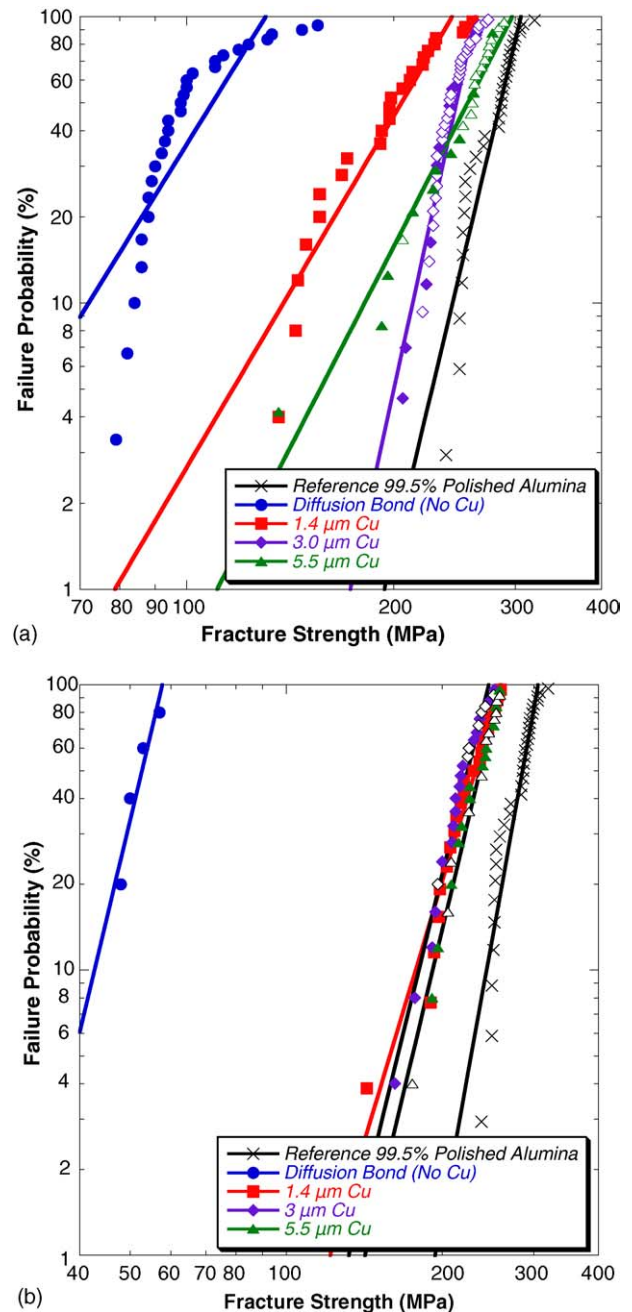


Fig. 7. Plots of fracture probability vs. fracture strength for alumina joined using Cu/Nb/Cu interlayers. Results are for bonding cycles of 6 h at 1400 °C using (a) polished substrates, and (b) as-ground (400 grit) substrates. It is evident that the liquid copper film is beneficial, especially for ground substrates.

mina blocks from the same source, but ground with a 400-grit wheel. AFM measurements over $50\ \mu\text{m} \times 50\ \mu\text{m}$ areas yielded R_a values of 0.027 and $0.154\ \mu\text{m}$ for the polished and as-ground surfaces, respectively. Both values are significantly less than the copper film thicknesses examined. Profilometry line scans over $50\ \mu\text{m}$ lengths provided an R_a of $0.011\ \mu\text{m}$ for the polished surfaces and R_a values of 0.213 and $0.247\ \mu\text{m}$ for the ground surfaces for scans parallel and perpendicular to the grinding direction, respectively. However, as the length scale of the measurement was increased to dimensions more comparable to the sample dimensions, 1 cm, significantly larger differences in the R_a became apparent. For the as-ground samples, R_a in scans parallel and perpendicular to the grinding direction increased to 0.299 and $2.72\ \mu\text{m}$, respectively. Over the dimensional scale of the bonding surface, large asperities and deep depressions, greater than $10\ \mu\text{m}$ in height or depth relative to the mean surface position, exist on the surface. The largest asperities will dictate the initial contact points and the initial separation distances between the ceramic and the core layer. This, in turn, will influence the pattern of liquid redistribution and film breakup. Although copper patches were noticeably larger and occupied a larger area fraction of the interface when ground substrates were used, the resulting mechanical properties, summarized in Fig. 7b, are encouraging. There appears to be a slight benefit to thicker films, perhaps reflecting more complete filling of the more severe interfacial gaps, but the overall properties are not significantly degraded in comparison to those of comparable joints made with polished substrates. The results suggest that the process is relatively forgiving, and useful for joining as-machined parts.

6. Summary and conclusions

TLP bonding provides an opportunity to join materials at reduced temperatures, which can be essential to preserving the performance of materials with temperature-sensitive microstructures. The results shown suggest that commercially available reactive-metal brazes coupled with low-melting-point cladding layers could be used to form joints at temperatures that are more commonly associated with soldering. TLP bonding relies on a substantial solid solubility of the low-melting-point component in a higher-melting-point host material, such as copper in platinum. This limits the candidate alloy systems. If the interdiffusion process leading to liquid disappearance involves substitutional diffusion, rather than the much more rapid interstitial diffusion (as for boron in nickel), joining times can be substantial. To reduce the time required for isothermal solidification, one must increase the bonding temperature (and diffusivity), or use thinner liquid films to reduce the amount of liquid former that must diffuse into the adjoining bulk material or core layer. Increasing the temperature counters the general desire to reduce processing temperature and protect temperature-sensitive components. Reducing the liquid thickness imposes increasingly stringent

surface preparation demands since there is likely to be insufficient liquid to fill large gaps at the interface. (Alternative methods of large gap filling rely on powder blends/slurries that more readily conform to the local topography.^{23–25})

These factors and considerations prompted efforts to devise and explore methods of joining that would exploit a higher diffusivity transport path at lower temperature. What emerged was a process that would exploit a liquid film, and rapid diffusion of the higher-melting-point metal within the liquid to facilitate joint formation. Disappearance of the liquid would not be required, merely rearrangement of the liquid phase so that the joint region no longer contained a continuous layer of the liquid former. By dispersing the liquid former, melting would have a minimal effect on the high-temperature properties of the joint. This alternative approach opened up a much wider range of alloy systems as interlayer candidates, ones in which the liquid former has minimal solubility in the host material.

The Cu/Nb/Cu interlayer system has served as a vehicle for numerous studies of liquid-film-assisted joining. The process can produce joints with reliably good properties, and high-temperature performance of the joints has been demonstrated. Assessments of phase diagrams suggest that there are many other candidate interlayer systems, some which provide much greater solubility of the core metal in the liquid. This could significantly increase the rate of ceramic-core layer growth provided that the interfacial energetics is appropriate. In addition, hybrids of TLP and LFAJ may also emerge.

Acknowledgements

This research was supported by the Director, Office of Science, Office of Basic Energy Sciences, Division of Materials Science and Engineering, of the U.S. Department of Energy under Contract No. DE-AC03-76SF00098. Takaya Akashi acknowledges support from a one-year fellowship from the Japanese Ministry of Education, Culture, Sports, Science and Technology. Sung Hong acknowledges support in the form of a Jane Lewis Fellowship. A.M. Glaeser wishes to thank the Japan Society for the Promotion of Science for an Invitation Fellowship for Research in Japan during which some of the ideas in this paper were formulated.

References

1. Nicholas, M. G. and Mortimer, D. A., Ceramic/metal joining for structural applications. *Mater. Sci. Technol. (UK)*, 1985, **1**(9), 657–665.
2. Loehman, R. E. and Tomsia, A. P., Joining of ceramics. *Am. Ceram. Soc. Bull. (USA)*, 1988, **67**(2), 375–380.
3. Sukanuma, K., Miyamoto, Y. and Koizumi, M., Joining of ceramics and metals. *Ann. Rev. Mater. Sci.*, 1988, **18**, 47–73.
4. Elssner, G. and Petzow, G., Metal/ceramic joining. *ISIJ Int.*, 1990, **30**(12), 1011–1032.
5. Brandon, D. and Kaplan, W. D., *Joining processes: an introduction*. John Wiley and Sons, New York, 1997.

6. Derby, B. and Wallach, E. R., Theoretical model for diffusion bonding. *Met. Sci. (UK)*, 1982, **16**(1), 49–56.
7. Derby, B. and Wallach, E. R., Diffusion bonding: development of theoretical model. *Met. Sci. (UK)*, 1984, **18**(9), 427–431.
8. Mulder, C. A. M. and Klomp, J. T., On the internal structure of Cu– and Pt–sapphire interfaces. *J. Phys.*, 1985, **46**(Suppl. C4), 111–116.
9. Hill, A. and Wallach, E. R., Modelling solid-state diffusion bonding. *Acta Metall.*, 1989, **37**(9), 2425–2437.
10. Reimanis, I. E., Pore removal during diffusion bonding of Nb–Al₂O₃ interfaces. *Acta Metall. Mater.*, 1992, **40**(Suppl.), S67–S74.
11. Dalgleish, B. J., Saiz, E., Tomsia, A. P., Cannon, R. M. and Ritchie, R. O., Interface formation and strength in ceramic–metal systems. *Scr. Metall. Mater.*, 1994, **31**(8), 1109–1114.
12. Bhadeshia, H. K. D. H., Joining of commercial aluminum alloys. In *Proceedings of International Conference on Aluminium (INCAL'03)*, ed. S. Subramanian and D. H. Sastry. 2003, pp. 195–204.
13. Klomp, J. T., Bonding of metals to ceramics and glasses. *Am. Ceram. Soc. Bull. (USA)*, 1972, **51**(9), 683–688.
14. Klomp, J. T. and Van De Ven, A. J. C., Parameters in solid-state bonding of metals to oxide materials and the adherence of bonds. *J. Mater. Sci.*, 1980, **15**(10), 2483–2488.
15. Dalgleish, B. J., Lu, M. C. and Evans, A. G., The strength of ceramics bonded with metals. *Acta Metall.*, 1988, **36**(8), 2029–2035.
16. Sukanuma, K., New process for brazing ceramics utilizing squeeze casting. *J. Mater. Sci.*, 1991, **26**(22), 6144–6150.
17. Duvall, D. S., Owczarski, W. A. and Paulonis, D. F., TLP bonding: a new method for joining heat resistant alloys. *Weld. J.*, 1974, **53**(4), 203–214.
18. Ikawa, H. and Nakao, Y., Transient liquid phase (T.L.P.) diffusion bonding of nickel-base heat resisting alloys. *Trans. Jpn. Weld. Soc.*, 1977, **8**(1), 3–8.
19. Ikawa, H., Nakao, Y. and Isai, T., Theoretical considerations on the metallurgical process in T.L.P. bonding of nickel-base superalloys. *Trans. Jpn. Weld. Soc.*, 1979, **10**(1), 24–29.
20. Nakao, Y., Nishimoto, K., Shinozaki, K. and Kang, C., Theoretical research on transient liquid insert metal diffusion bonding of nickel base alloys. *Trans. Jpn. Weld. Soc.*, 1989, **20**(1), 60–65.
21. MacDonald, W. D. and Eagar, T. W., Transient liquid phase bonding. *Ann. Rev. Mater. Sci.*, 1992, **22**, 23–46.
22. Zhou, Y., Gale, W. F. and North, T. H., Modelling of transient liquid phase bonding. *Int. Mater. Rev.*, 1995, **40**(5), 181–196.
23. Gale, W. F., Wen, X., Zhou, T. and Shen, Y., Microstructural development and mechanical properties of wide gap and conventional transient liquid phase bonds between Ti–48Al–2Cr–2Nb substrates. *Mater. Sci. Technol. (UK)*, 2001, **17**(11), 1423–1433.
24. Gale, W. F. and Wen, X., Ni₃Al based composite interlayers for wide gap transient liquid phase bonding of NiAl–Hf single crystals to a nickel base superalloy. *Mater. Sci. Technol. (UK)*, 2001, **17**(4), 459–464.
25. Gale, W. F., Butts, D. A., Di Ruscio, M. and Zhou, T., Microstructure and mechanical properties of titanium aluminide wide-gap, transient liquid-phase bonds prepared using a slurry-deposited composite interlayer. *Metall. Mater. Trans. A Phys. Metall. Mater. Sci.*, 2002, **33**(10), 3205–3214.
26. Shalz, M. L., Dalgleish, B. J., Tomsia, A. P., Cannon, R. M. and Glaeser, A. M., Ceramic joining III. Bonding of alumina via Cu/Nb/Cu interlayers. *J. Mater. Sci.*, 1994, **29**(14), 3678–3690.
27. Shalz, M. L., Dalgleish, B. J., Tomsia, A. P. and Glaeser, A. M., Ceramic joining I. Partial transient liquid-phase bonding of alumina via Cu/Pt interlayers. *J. Mater. Sci.*, 1993, **28**(6), 1673–1684.
28. Shalz, M. L., Dalgleish, B. J., Tomsia, A. P. and Glaeser, A. M., Ceramic joining II. Partial transient liquid-phase bonding of alumina via Cu/Ni/Cu multilayer interlayers. *J. Mater. Sci.*, 1994, **29**(12), 3200–3208.
29. Marks, R. A., Sugar, J. D. and Glaeser, A. M., Ceramic joining IV. Effects of processing conditions on the properties of alumina joined via Cu/Nb/Cu interlayers. *J. Mater. Sci.*, 2001, **36**(23), 5609–5624.
30. Dalgleish, B. J., Tomsia, A. P. and Glaeser, A. M., Transient liquid phase bonding of silicon ceramics via microdesigned Ni-based interlayers. *Ceram. Trans.*, 1994, **46**, 555–566.
31. Dalgleish, B. J., Tomsia, A. P. and Glaeser, A. M., A transient FGM approach to joining Si-based ceramics. In *Proceedings of FGM-94*, ed. N. Cherradi and B. Ilschner. Presses Polytechnique et Universitaires Romandes, Lausanne, 1995, pp. 503–508.
32. Locatelli, M. R., Tomsia, A. P., Nakashima, K., Dalgleish, B. J. and Glaeser, A. M., New strategies for joining ceramics for high-temperature applications. *Key Eng. Mater.*, 1995, **111–112**, 157–190.
33. Ceccone, G., Nicholas, M. G., Peteves, S. D., Tomsia, A. P., Dalgleish, B. J. and Glaeser, A. M., An evaluation of the partial transient liquid phase bonding of Si₃N₄ using Au coated Ni–22Cr foils. *Acta Mater.*, 1996, **44**(2), 657–667.
34. Nakashima, K., Mori, K. and Glaeser, A. M., Wettability of Cu-based alloys on alumina and joining of alumina with microdesigned nickel–chromium alloy interlayers. In *Ceramic microstructures: control at the atomic level*, ed. A. P. Tomsia and A. M. Glaeser. Plenum Press, New York, 1998, pp. 407–414.
35. Nakashima, K., Makino, T., Mori, K. and Glaeser, A. M., Wettability and interfacial reaction between Si₃N₄ and Cu-based alloys. *Key Eng. Mater.*, 1999, **159–160**, 287–292.
36. Dalgleish, B. J., Tomsia, A. P., Nakashima, K., Locatelli, M. R. and Glaeser, A. M., Low temperature routes to joining ceramics for high-temperature applications. *Scr. Metall. Mater.*, 1994, **31**(8), 1043–1048.
37. Dalgleish, B. J., Nakashima, K., Locatelli, M. R., Tomsia, A. P. and Glaeser, A. M., New approaches to joining ceramics for high-temperature applications. *Ceram. Int.*, 1997, **23**(4), 313–322.
38. Locatelli, M. R., Marks, R. A., Chapman, D. R., Nakashima, K. and Glaeser, A. M., Transient liquid phase (TLP) routes to the joining of structural ceramics. In *Interfacial science in ceramic joining*, ed. A. Bellosi, T. Kosmac and A. P. Tomsia. Kluwer Academic Publishers, Dordrecht, The Netherlands, 1998, pp. 111–134.
39. Sugar, J. D., McKeown, J. T., Marks, R. A. and Glaeser, A. M., Liquid-film-assisted formation of alumina/niobium interfaces. *J. Am. Ceram. Soc. (USA)*, 2002, **85**(10), 2523–2530.
40. Massalski, T. B., Okamoto, H. and ASM International, *Binary alloy phase diagrams (2nd ed.)*. ASM International, Materials Park, Ohio, 1990.
41. Nogi, K., Oishi, K. and Ogino, K., Wettability of solid oxides by liquid pure metals. *Mater. Trans. JIM (Jpn.)*, 1989, **30**(2), 137–145.
42. Nikolopoulos, P., Agathopoulos, S. and Tsoga, A., A method for the calculation of interfacial energies in Al₂O₃ and ZrO₂ liquid–metal and liquid–alloy systems. *J. Mater. Sci.*, 1994, **29**(16), 4393–4398.
43. Marks, R. A., Chapman, D. R., Danielson, D. T. and Glaeser, A. M., Joining of alumina via copper/niobium/copper interlayers. *Acta Mater.*, 2000, **48**(18–19), 4425–4438.
44. Kruzic, J. J., Marks, R. A., Yoshiya, M., Glaeser, A. M., Cannon, R. M. and Ritchie, R. O., Fracture and fatigue behavior at ambient and elevated temperatures of alumina bonded with copper/niobium/copper interlayers. *J. Am. Ceram. Soc. (USA)*, 2002, **85**(10), 2531–2541.